Proceedings of ASME Turbo Expo 2011
GT2011
June 6-10, 2011, Vancouver, British Columbia, Canada

GT2011-45931

ENDWALL CONTOURING USING CONTINIOUS DIFFUSIION, A BREAKTHROUGH METHOD AND ITS APPLICATION TO A THREE-STAGE HIGH PRESSURE TURBINE

M.T. Schobeiri, K. Lu
Turbomachinery Performance and Flow Research Laboratory
Texas A&M University
Phone: (979)845-0819, Fax: (979)845-3081
tschobeiri@tamu.edu

ABSTRACT

Blades of high pressure turbines have a relatively small aspect ratio that produce major secondary flow regions close to the hub and tip. The secondary flows caused by a system of hub and tip vortices induce drag forces resulting in an increase of secondary flow losses and thus a reduction of stage efficiency. Given the high level of technological maturity and the current state of turbine aerodynamic efficiency, major efficiency improvement, if any, can be achieved only by significant R&D effort. In contrast, moderate increase in aerodynamic efficiency is attainable by reducing the effect of parasitic vortices such as those mentioned above. Introducing an appropriate non-axisymmetric endwall contouring reduces the secondary flow effect caused by the pressure difference between pressure and suction surfaces. Likewise, attaching leading edge fillets reduces the strength of horse shoe vortices. While an appropriate endwall contouring design requires special care, the design of the leading edge fillet is straight forward. In this paper we present a physics based method which enables researchers and engineers to design endwall contours for any arbitrary blade type regardless of the blade loading, degree of reaction, stage load and flow coefficients. A thorough step-by-step design instruction is followed by its application to the second rotor of the three-stage research turbine of Turbomchinery Performance and Flow Research Laboratory (TPFL) of Texas A&M University. Comprehensive numerical calculations of the flow field including the secondary flow show the positive impact of an appropriately designed endwall contouring on the efficiency. The results also show, how an inappropriately designed contour can be detrimental to turbine efficiency. The numerical result of the efficiency calculations is compared with the experimentally obtained efficiency for the reference non-contoured turbine.

NOMENCLATURE

C_{ax}	Axial chord length of the blade
HP, IP, LP	High, intermediate, low pressure
h_{ip}	height of the pressure side of the i_{th} diffuser section
h_{is}	height of the suction side of the i_{th} diffuser section
L_i	Length of the i_{th} diffuser section
p_i	static pressure
U_p, U_s	diffuser inlet and exit velocity outside the boundary layer
R_h	hub radius
γ	blades stagger angle
δ	boundary layer thickness
σ	cascade solidity, $\sigma=c/s$
λ	diffuser recovery factor

$$\lambda=\frac{\Delta p_i}{\frac{1}{2}\rho U_p^2}=1-\frac{\left(\Delta h_i\right)_p^2}{\left(\Delta h_i\right)_s^2}$$

INTRODUCTION

The HP-turbine, in contrast to LP-turbine, has a relatively small aspect ratio which causes major secondary flow regions close to the hub and tip. As a result, the secondary flow caused by a system of hub and tip vortices that induce drag forces resulting in an increase of secondary flow losses, as extensively discussed in [1]. Focusing on the secondary flow loss mechanisms, the fluid particles within the endwall boundary layers are exposed to a pitchwise pressure gradient in the blade channel. The particles move from the pressure side to the suction side and generate a system of vortices. These vortices induce drag forces that are the cause of the secondary flow

losses. In addition, their interaction with the main flow causes angle deviation inside and outside the blade channel, resulting in additional losses due to angle deviation. The nature of different flow losses is comprehensively treated in the classical work of Traupel [2]. Schobeiri [1] dedicated a full chapter of his book to the physics of loss generation and its calculation. Denton [3] summarized the loss mechanisms. Further reviews of the subject matter were provided by Sieverding [4] and Langston [5].

The secondary flow loss is almost inversely proportional to the aspect ratio [1]. Thus, in HP-turbines with small aspect ratios, the secondary flow loss of almost 40-50% is the major loss contributor. It can be reduced by introducing the following measures:

(1) Three-Dimensional compound lean design.
(2) Special design for turbines that are subjected to extreme off-design incidence change
(3) Modification of the blade leading edge using fillets
(4) Endwall contouring
(5) Hub cooling mass flow injection to interact with the hub secondary flow
(6) Blade tip cooling ejection to reduce the tip secondary flow losses

3-D Compound Lean: One of the efficient methods of reducing the secondary flow zone is utilizing the compound lean blade design that reduces the secondary losses by varying the lean angle, [1]. The effectiveness of the 3-D leaned design in suppressing the secondary flow is demonstrated in efficiency and performance studies by Schobeiri and his co-workers, among others [6] and [7]. A subsequent comparative study [8] using cylindrical blades with identical blade height, hub and tip diameter, and inlet conditions revealed a significant efficiency improvement close to $\Delta\eta \approx 2\%$ for the rotor with the 3-D compound lean blades compared to the one with cylindrical blades. This significant efficiency improvement was due to a major reduction in secondary flow losses.

Blade for Extreme Off-design Operation: In a recent paper Schobeiri and his co-workers [9] showed that by designing turbines with almost zero pressure difference over first 50% of the axial chord, the secondary flow can be eliminated. The combination of zero secondary flow and a moderate leading edge radius created a turbine blade that is insensitive with respect to an incidence change of $\pm 30°$.

Fillets: Investigations by Sauer and Wolf [10], [11] and the subsequent study by Sauer et al. [12] have shown that the secondary flow losses of a turbine cascade could be reduced by modifying the leading edge profile of an inlet stator vane at the transition from the wall into the leading edge. Zess and Thole [13] performed both computational design and experimental validation of a fillet placed at the leading edge-endwall juncture of a guide vane to eliminate the horseshoe vortex. The fillet design effectively accelerated the incoming boundary layer thereby eliminate the horseshoe vortex. The results of this study also showed significant reductions in the turbulent kinetic energy levels and in the streamwise vorticity levels. Using leading edge bulbs, and a leading edge fillet Becz et al. [14] have shown that both the small bulb and fillet geometries each reduced area averaged total loss by 8%, while the large bulb exhibited a slight increase in total loss. One of the measures to improve the turbine efficiency is the endwall contouring. Focusing on the impact of endwall contouring in the turbine efficiency, we present a physics based method which enables researchers and engineers to design endwall contours for any arbitrary blade type regardless of the blade loading, degree of reaction, stage load and flow coefficients. To emphasize the characteristic differences between the present method and those available in the literature, a brief review of existing research work is presented in the following.

ENDWALL CONTOURING

In recent years, numerous papers have been published that deal with the effect of endwall contouring and leading edge filleting. With a few exceptions of rotating rig investigations that deal with the endwall contouring of LP-turbines, most of the published studies are either numerically or experimentally performed in turbine cascades with steady inlet flow conditions. Numerical and experimental studies by [15], [16], [17] and [18] show a reduction of total pressure losses by as much as 50%.

Cascade Endwall: The papers discussed in this section represent a few among many that are dealing with the impact of endwall contouring on turbine endwall secondary flow.

Experimental and numerical cascade flow study by Ingram et al. [19] showed the influence of end-wall profiling. The best end-wall profile tested has shown a 24% reduction in the secondary loss. Further investigations by Ingram et al. [20] designed a new 'aggressive' profiling of the end wall to produce a large reduction in loss possible. However, the experimental results, showed an increase of secondary flow loss. Saha and Acharya [21] combined two curves, one that varies in the streamwise direction while the other varies in the pitchwise direction. They created several contoured end-walls by varying the streamwise variation keeping the pitchwise curve constant. The results show that the contoured end-wall can reduce the secondary flow by decreasing radial pressure gradient.

Praisner et al. [22] studied the application of non-axisymmetric endwall contouring to mitigate the endwall losses of front- and aft loaded turbine baldes. With flat endwalls, the front-loaded design showed significantly higher secondary losses than the aft-loaded and the reference conventional blades. To contour the endwall they used two-dimensional cubic splines in both the pitch- and stream-wise directions along the endwall. The predicted loss reduction for the front loaded airfoil design was at 12% while the measured loss reduction was twice as high at 25%. The predicted and measured loss reductions for the reference blade were 4% and 10% respectively while a 5% row-loss reduction was predicted for the aft-loaded blade. The comparison between the CFD and experiments reveals that, while the CFD calculations predict the trends of flow modifications with endwall contouring, they lack a significant level of accuracy for individual flow features

such as the passage vortex. Harvey et al. [23] and Hartland, et al. [24] modified the end wall for the large-scale, low-speed rotor profile in a linear cascade. The end wall surface was created by the product of two curves in axial and circumferential directions. The axial profile was defined by a B-spline curve through six control points. The first three terms in the Fourier series were used to produce the perturbations in the circumferential direction. They reported a measured net total loss reduction by 20% and the net secondary loss by 30%. The CFD losses show little change. The experimental data show mixed-out losses, where the reductions with the profiled end wall were 15% in net total loss and 34% in secondary loss.

Rotating Turbine: In contrast to the tremendous multitude of the cascade endwall papers, from which only a few have been discussed above, there are only a few investigations of the impact on endwall contouring in rotating turbines. Brennan et al. [25] redesigned the HP turbine of the Rolls-Royce Trent 500 engine with the application of non-axisymmetric end walls. The profiled end-wall shape was determined by six control stations which were fixed at specified axial distances along the mean camber line of the airfoil. The addition of profiling to the end-walls of the HP Turbine is predicted to reduce secondary loss by 0.24% of the NGV and by 0.16% for the Rotor. The total improvement in stage efficiency for the HP Turbine is therefore +0.4%.

Harvey et al. [26] redesigned the IP-turbine stager by applying non-axisymmetric end walls to both the vane and blade passages. They reported an improvement in the stage efficiency of 0.9 ± 0.4% at the design point. Germain et al. [27] studied the improvement of efficiency of a one-and-half stage high work axial flow turbine by non-axisymmetric endwall contouring. The endwalls have been designed using automatic numerical optimization by means of a Sequential Quadratic Programming (SQP) algorithm. Both hub and tip endwalls of the first stator as well as the hub endwall of the rotor were modified. The experimental results confirm the improvement of turbine efficiency, showing a total-total stage efficiency benefit of 1%±0.4%, while the improvement is underestimated by CFD. Snedden et al. [28] and [29] utilized 5-hole probe measurements in a 1.5 stage low speed, model turbine in conjunction with computational fluid dynamics to gain a more detailed understanding of the influence of a generic endwall design. Results indicated a 0.4% improvement in total-total rotor and stage efficiency as a result of the application of the generic non-axisymmetric endwall contouring. However, at higher loading the rotor efficiency was reduced by 0.5%.

NECESSITY OF TURBINE RIG INVESTIGATIONS

The above cascade studies indicate that, based on the cascade loading, the endwall contouring positively influences the secondary flow reduction. However, these studies do not consider the effects of rotation, rotor- stator interaction, periodic unsteady wakes and their impact on the boundary layer transition of the following blade rows. Furthermore, the lack of centrifugal and Coriolis forces that are inherent to a rotating turbine, raises questions as to what extent the cascade results are transferable to a rotating turbine environment. Comprehensive turbine rig experimental studies at the TPFL show a major qualitative and quantitative difference between turbine rig and cascade results. In addition, as shown in [6] and [7], a substantial increase in secondary flow losses is observed when the turbine operates at off-design rotational speeds or off-design mass flows. Because of the absence of rotating effects in stationary cascades, discussed above, it seems unlikely that the stationary cascade investigations would produce results that can be transferred to engine conditions. Considering this circumstance, extensive numerical simulations were performed to find an optimum method of endwall contouring to be applied to a three-stage turbine before an expensive hardware modification is performed for experimental verification.

Numerical Analysis, Grid Sensitivity: As extensively discussed in [30], the deficiencies in turbulence and transition models that cause major differences in efficiency calculations compared with the experiment, suggest that caution should be exercised, when interpreting numerical results. Therefore, the numerical results generated under these circumstances are of qualitative nature only. In performing parameter variations, however, the numerical simulation predicts the trends satisfactorily. For our turbine rig application shown in Fig.1, extensive verifications and possible rectifications of the existing methods were essential before producing hardware to be tested. This required extensive numerical studies to determine the impact of the above methods on the turbine rig flow field including pressure, velocity, vorticity, total pressure loss distributions and the turbine efficiency. We numerically simulated several cases. For each individual case several grids were generated to ensure the results were grid insensitive, Fig.2. By performing the grid sensitivity analysis, we refined the grid density until we achieved a constant efficiency for the entire turbine rig. This is imperative, whenever the efficiency verification is the most important outcome as is in this study. The efficiency convergence required for the rotor a mesh with over 2 million elements, 22 nodes at the wall region and 9 million elements for the entire model. For each single case a parallel computation on A&M Super Computers took more than hundred hours of computation time. For numerical simulation the commercial code CFX with SST-turbulence model was used. Extensive turbulence model studies performed on several TPFL-turbines and the numerical calculation showed the suitability of SST-model for calculating the flow quantities. For each of the calculated cases, the entire flow field including total pressure loss and the turbine efficiency were obtained. Particular attention was paid to accurately obtaining the efficiency of the turbine with the second rotor endwall contoured. Following the conventional approach applied the three-stage TPFL-HP-turbine blading shown in Fig.1, an example is given in Fig. 3, where the peak is placed on the pressure side of the turbine, while varying its height and the axial position. Several fifth order polynomials were applied to define the variation of contour height and axial position in streamwise direction as shown in Fig.4. The figure shows

configurations with (a) a contouring that is raised above the hub and occupies only a portion of the hub surface, called positive

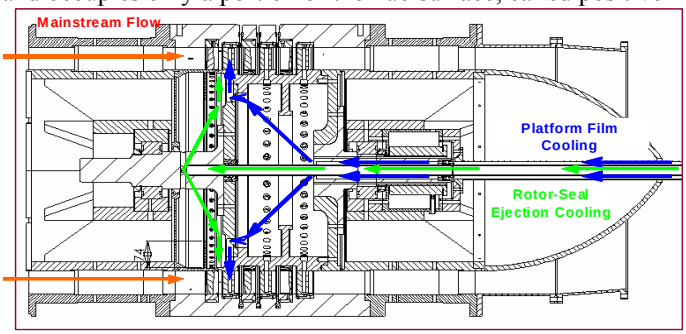

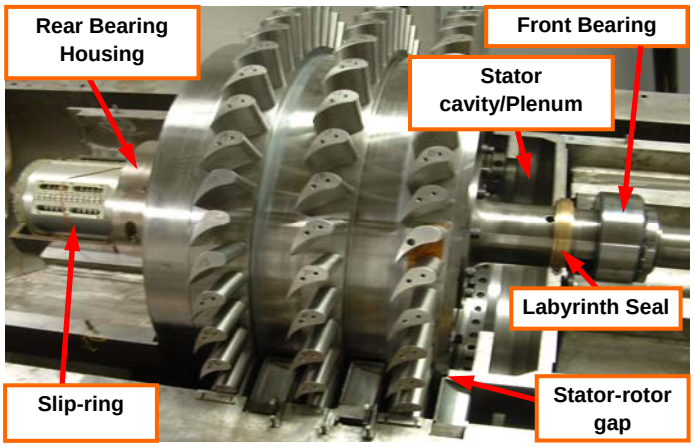

Fig. 1: Top, Details of the new Rotor; bottom: the three-stage rotor

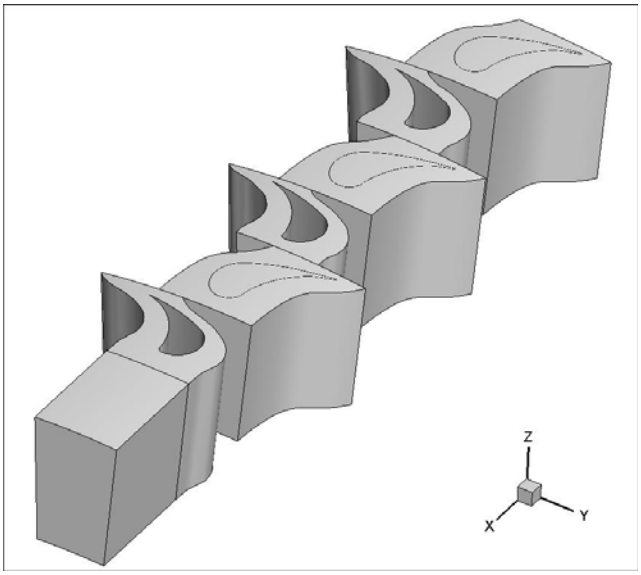

(a)

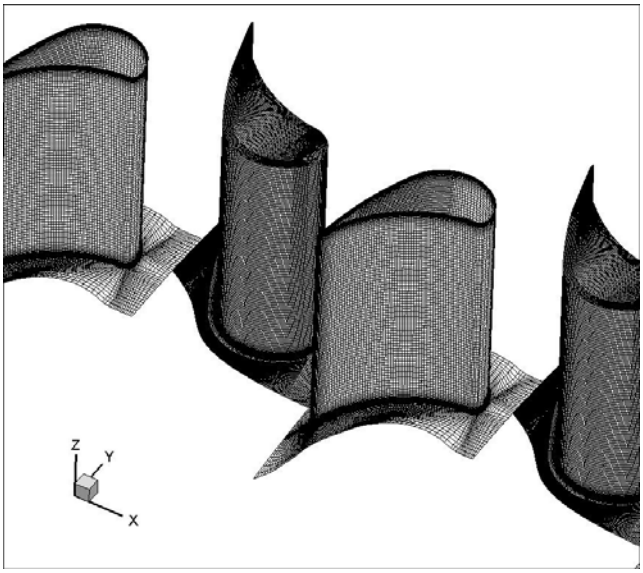

(b)

Fig. 2: (a) Row-by-row configuration; (b) CFD mesh

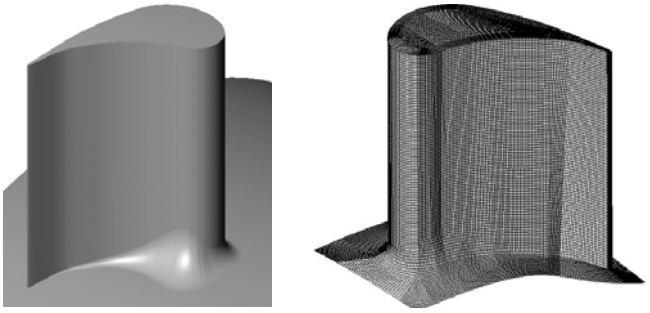

Fig.3: Contouring using the conventional method

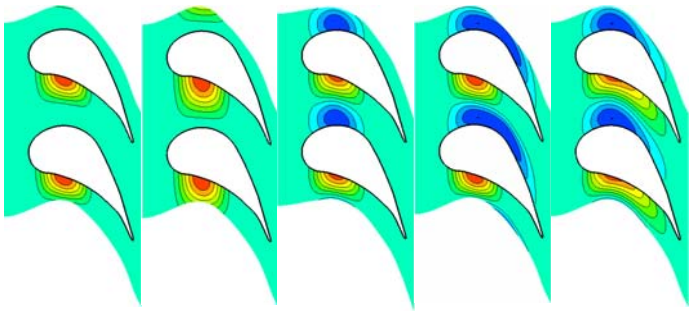

(a) (b) (c) (d) (e)

Fig. 4: Contour variation: (a) partial positive contouring; (b) extended partial positive contouring, (c) partial positive, negative contouring; (d) extended partial positive, negative contouring; (e) full passage contouring. The maximum positive height for all cases is 6 mm, the minimum negative height is -3mm

contouring, (b) a contouring that is raised above the hub surface but is circumferentially extended towards the suction surface, called extended partial positive, (c) a contouring with a portion that is raised above the hub followed by a portion that is lowered into the hub surface, called partial positive, negative contouring, (d) as (c) but with extended negative part and finally (e) a contouring with extended positive and negative portions that occupy the entire passage, called full passage contouring. Efficiency calculation results of the second rotor for different contouring used in this study are shown in Fig. 5.

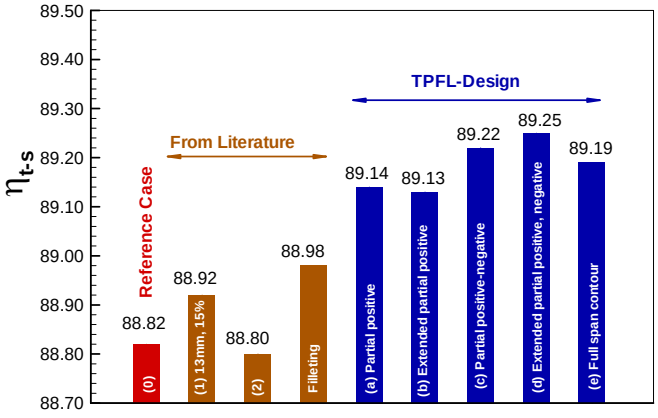

Fig. 5: Efficiency chart of numerically investigated cases

Using the conventional approach, several cases were numerically simulated, where the peak height and its axial location were systematically varied. After variation of the height, the peak height was kept constant at 13mm, while its axial location was varied from 15% to 30% of the axial length. As representative examples, Fig. 5 shows the efficiency calculation results labeled with (1) and (2). In addition, the filleting was also implemented into the catalog of simulations. Assuming an optimal position of the height within the range of 10%-15%, new contour shapes were introduced to perform an optimization process with the efficiency as the objective function. For each case a new grid was generated, numerical simulations performed and the efficiency results presented in Fig. 5 labeled with (a) through (e). As the results in Fig.5 show, using the trial and error approach associated with optimization process that was implemented into the numerical process has not delivered a trend toward an optimum solution. Furthermore, it was shown that the efficiencies were inconsistent throughout and the results were inconclusive to be transferred to different turbine blade types. Most importantly, the method used in the publically available literature is not suitable to provide a generalized design guideline for the research and design community. This circumstance motivated the lead author to introduce a new and physics based method to effectively design endwall contouring for any type of blading regardless its application to HP-, IP- or LP- turbine.

NEW ENDWALL CONTOURING

Turbine blades designed for applications in power generation and aircraft gas turbines as well as in steam turbines have in general different specific stage load coefficients, flow coefficients and degree of reaction. Furthermore, they are twisted from hub to tip to account for a prescribed radial equilibrium. The stator and rotor row for each turbine type have different solidity, aspect ratio and Zweifel number. In addition, the blades with the same inlet and exit flow angles might have different pressure distributions on pressure and suction surfaces (front- or aft- loaded). In this section we develop a step-by-step physics based method for endwall contouring that can be recommended to the turbine design community as a guideline.

Continuous Diffusion Method for Endwall Contouring

The method utilizes a continuous prescribed deceleration of the secondary flow velocity from pressure to suction surface by a diffuser type of flow path that is thought of a number of narrow diffusers with the width ΔW_i, a given inlet height and variable exit heights that produce a desired target pressure. The diffuser raises the pressure on the endwall suction side thus reducing the secondary flow velocity, the strength of the secondary vortices, the associated induced drag forces and the total pressure loss due to the latter. The method can be applied to HP-, IP-, and LP- turbines and compressors regardless the load coefficient, flow coefficient and degree of reaction. It is strongly physics based, very straight forward and easy to use. The following step-by-step instruction presents a tool for appropriately designing non-axisymmetric contours:

1) For the reference non-contoured blade place a cylindrical control surface at a radius $R_{hub}+\delta$ with δ as the boundary layer thickness developed by the secondary flow from the pressure to the suction side, Fig. 6 (A). The boundary layer thickness can easily be estimated, [30]
2) For the reference blade obtain the pressure distribution on hub, Figure 6(B).
3) For the reference (non-contoured) blade find the actual distribution of the pressure difference Δp_i between the pressure and the suction surface and define a target pressure difference $\Delta p_{target} > \Delta p_{lim}$ with Δp_{lim} as the minimum pressure difference, below which, the diffuser flow will separate. Ideally the target pressure should be close to zero. This, however, will lead to a large area ratio for the local diffuser and thus a flow separation. The attached diffuser performance, Fig. 6D allows designing an appropriate diffusion path with an optimal performance.
4) Obtain the topology of streamlines at the same radial position, sketched in Fig. 6(C1) based on Fig.7. This step determines the local velocity vector pertaining to each streamline. This combined with step 5 provides the input to construct the diffuser channels that follow the streamlines. Another alternative is decomposing the velocity vector into axial V_{ax} and circumferential V_u (pitchwise) components. This allows using V_u for constructing diffuser channels that follow the pitchwise velocity component, Fig. 6(C2). Both alternatives are equally applicable, however the latter has the advantage of extending the diffuser channels slightly upstream of the leading edge and downstream of the trailing edge.

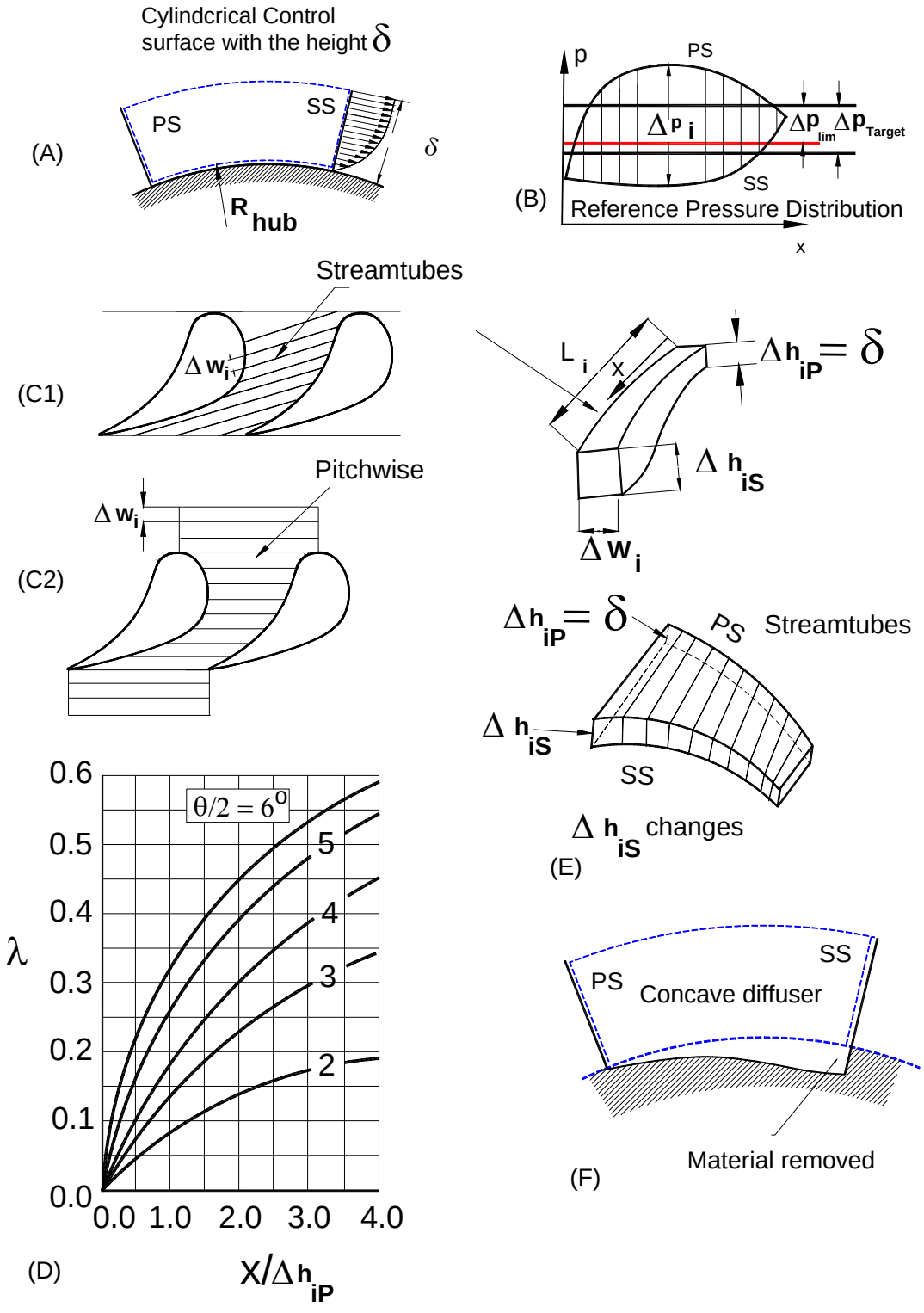

Fig.6: Explaining the continuous diffusion process for designing physics based endwall contouring

5) Starting with a constant ΔW_i for example $\Delta W_i = 0.05 C_{ax}$, choose a pressure recovery factor λ on the suction surface, for example $\lambda = 0.6$, by which the flow is still attached. This λ is taken from [31], where a series of diffuser performance maps for different diffuser-length/inlet-height ratios corresponding to $x/\Delta h_{ip}$ are presented. Figure 6D schematically represents one of those diagrams. With this λ, then calculate the contour height Δh_{is} on the suction surface that establishes a pressure difference Δp defined in nomenclature that we set equal to Δp_{target}. Using this target pressure, the diffuser can be constructed, Fig. 6(E), with the constant $\Delta h_{ip} = \delta$ at the pressure side and variable $\Delta h_{is} > \delta$ at the suction side from leading edge to trailing edge, Fig. 6(D).
6) Design the 3-D contour by removing the hub material, Fig. 6(F). A decay function at the inlet and the exit ensures a smooth transition of the contour.
7) Make sure that the throat integrity is not affected, this can be checked by using the mass flow balance.
8) Generate a high density grid for the above design and run CFD with SST-turbulence model.
9) Re-evaluate the results and make changes if necessary. An "aggressive" endwall design may require a complete re-design of the entire stage.

RESULTS AND DISCUSSIONS

Pressure Distribution

The new method is applied to the second rotor of the TPFL-HP-turbine, where steps 1 through 7 are executed. The critical range which was captured by the streamlines shown in Fig. 7 extends from 17% to 55%. Figures 8 shows the construction of the new endwall contours compared to the reference case. It is followed by Fig. 9, which displays the streamlines for both cases. In addition to reducing the secondary flow, Fig. 9 shows a substantial weakening of the incoming horseshoe vortices.

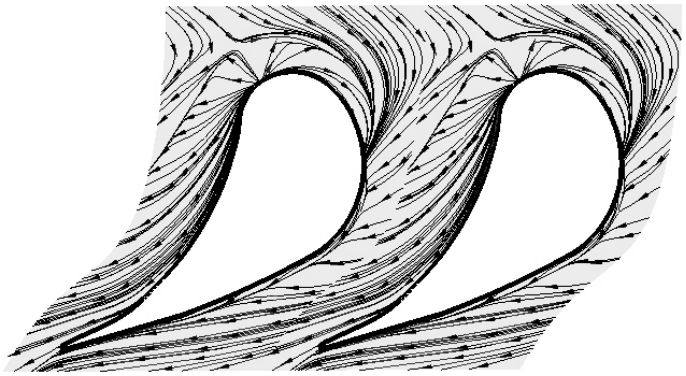

Fig. 7: Streamlines from suction to pressure surface used for construction the diffusion channel

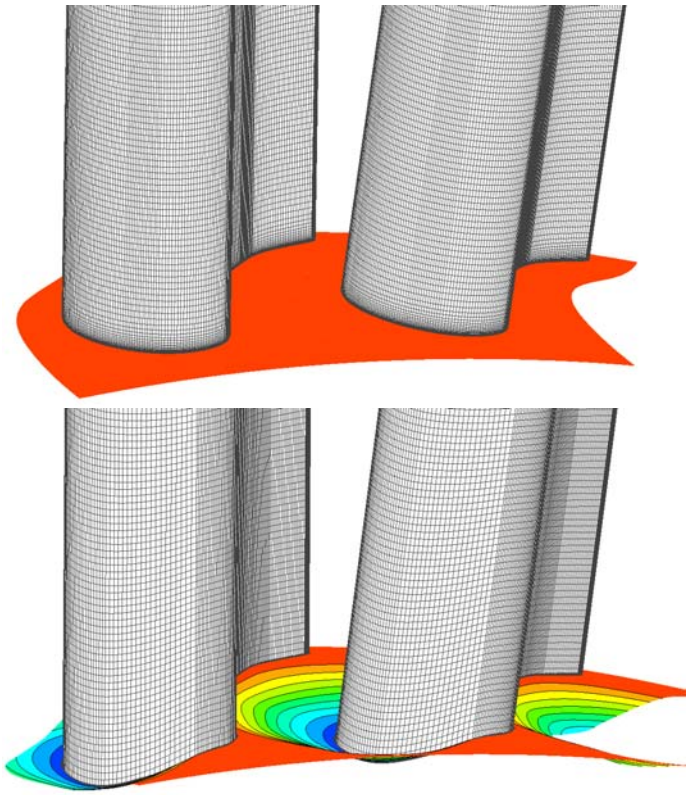

Fig. 8: Non-contoured (top), new contouring method (bottom)

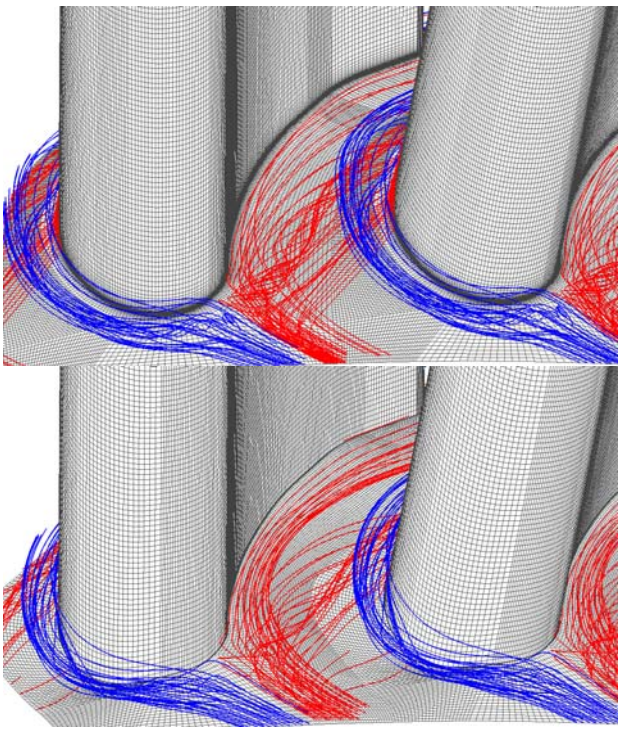

Fig. 9: Streamlines for reference case (top) and new contouring (bottom)

Figure 10 shows the pressure distribution directly on the hub. A target pressure is constructed and the corresponding height distribution Δh_{is} was calculated using the diffuser performance map by setting λ=0.6. This allows a pressure recovery close to the separation point. With the Δh_{is}-distribution implemented into the hub of the second rotor, a high density grid was generated for the entire turbine. The subsequent numerical simulation delivered the stage flow quantities, among other things, the new pressure distribution on the hub. Figure 10 shows a major shift of the suction surface pressure toward the pressure surface with a maximum value of 1600 Pa and a minimum of 800 Pa. As shown, in the target pressure range, the suction surface pressure covers exactly the prescribed target pressure. From about 6% to 17% and from 55% to about 73% there are still substantial pressure gains on the suction surface reducing the suction effect. Upstream of 6% and downstream of 73%there are pressure decreases on the suction side. These can be also eliminated by extending the target pressure to upstream of 17% and downstream of 73%.

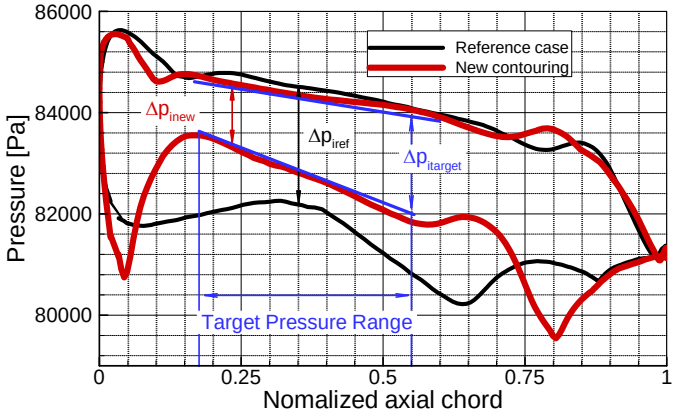

Fig. 10: Pressure distribution directly on the hub, a target pressure is set the diffusion channel constructed that leads to endwall contouring, Black line: the reference case, redline the new pressure distribution.

Figure 11 compares three different cases: (1) the reference case, (2) the conventional case using extended partial positive (+6 mm) and extended partial negative (-3mm) shown in Fig. 4d and the new case. The conventional case is effective only in a very narrow range close to the leading edge. Its effectiveness diminishes, when moving from this region away toward the leading and the trailing edge. Its effectiveness diminishes completely when moving just a few millimeters from the hub surface as shown in Fig. 12. It should be pointed out that the secondary vortices in this and the reference case extend above 2% spanwise.

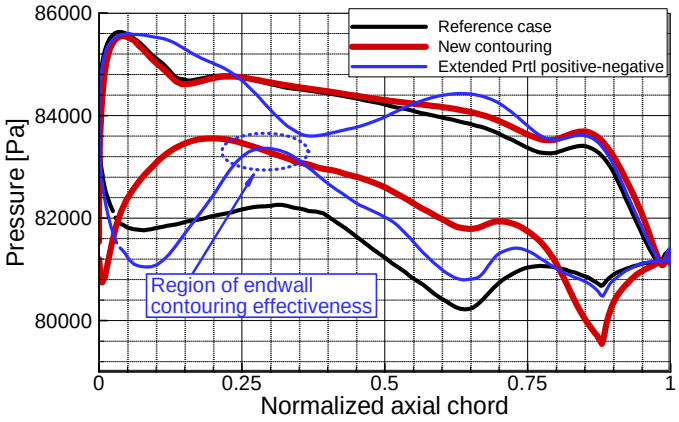

Fig. 11: Pressure distributions on the hub

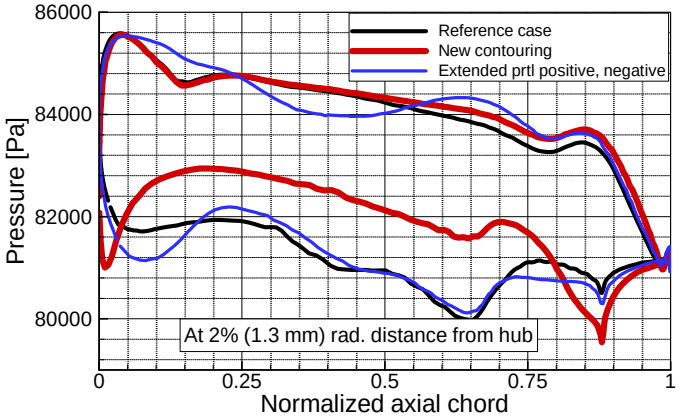

Fig. 12: Pressure distributions above the hub

A clear picture of the impact of the endwall contouring on the pressure distribution is seen in Fig. 13. In the reference case (a) close to the axial location of about 28%, where the maximum positive height is located, with the exception of a wake-like pattern that is caused by the incoming horseshoe vortices, the isobars have more or less an orderly stable pattern. In pitchwise direction, however, a strong pressure gradient fieled dominates the flow picture from the leading to the trailing edge. Keep in mind that the purpose of the endwall contouring has been to weaken this pressure gradient field. The extended partial positive-negative case (b) seems to only perturb the pressure field locally. This is quite consistent with the pressure distribution shown in Fig. 11. A more orderly pattern of isobars associated with a much weaker pressure gradient is seen in Fig. 13(c) of the new contouring.

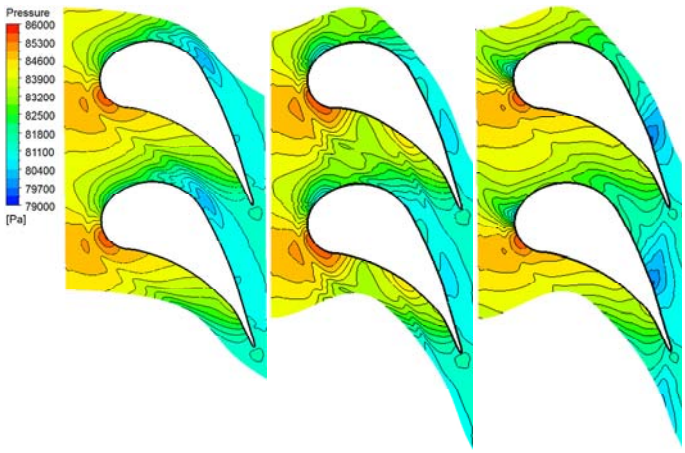

(a) Reference case (b) Extended partial positive, negative (c) New contouring

Fig. 13: Contour plots of pressure distributions

Efficiency and Secondary Loss

The efficiency calculation for the second rotor with the new endwall contour is presented in Fig. 14. As seen the, the new method has brought an increase of $\Delta\eta$ = 89.33-88.82 = 0.51%. This increase is quite remarkable given the fact that we defined our target pressure such that it covers the critical range of 38% of the axial length. Moreover, it has exceeded all the other values delivered by the conventional trial and error method discussed earlier. Further efficiency improvement is expected by extending the target pressure upstream of 6% and downstream of 73%.

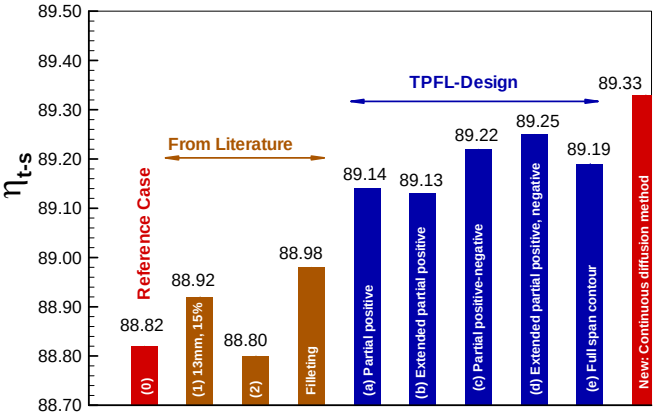

Fig. 14: Efficiency chart of all investigated wall contours

Figure 15 displays the total pressure loss coefficient for the reference case, the case with extended partial positive, negative and the new endwall contour. For the new contour, the integration of the loss coefficients resulted in a reduction of secondary flow loss relative to the reference case of $\Delta\zeta_R$ = 27.9%. In contrast, in case of the extended partial positive-negative has caused an increase in relative secondary flow loss of $\Delta\zeta_R$ = 6.3%. Considering the calculated second rotor efficiency of 89.25% which is higher than the reference efficiency of 88.82%, Fig. 14, one may conclude that the increase of the secondary flow loss coefficient and the increase of the efficiency are contradicting each other. However, this is not the case for two reasons: (1) A relative loss coefficient increase of 6.3% has only a marginal impact on the absolute value of the rotor efficiency, (2) when calculating the rotor efficiency the entire aero-thermodynamic quantities are involved that includes total temperature, total pressure and the static pressure.

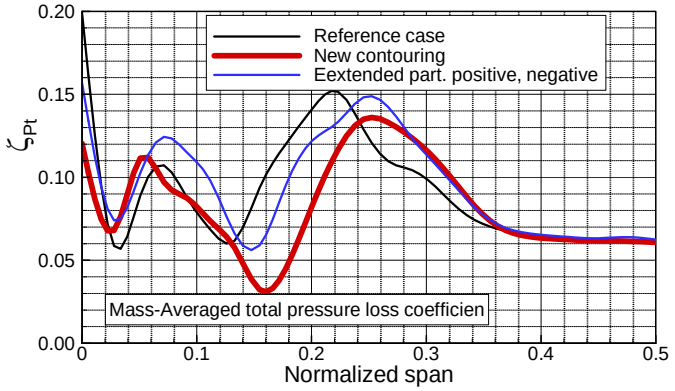

Fig. 15: Total pressure loss coefficients for Reference case, new contouring and extended partial positive, negative

FLOW STRUCTURE

Vorticity Distribution

Very close to the hub, the dominance of the pressure gradient from the pressure to suction surface causes the fluid particles to move pitchwise and produce a system of vortices. Figure 16 shows the vorticity distributions at three axial positions. The left column with three figures pertains to the reference (non-contoured) case. For the 30% C_{ax} case, the onset of the vortex seems to locate in between the suction and the pressure surface. It extends to the suction surface, where its strength becomes a maximum. Moving in axial direction its onset moves further toward the suction surface. Close to 55% axial location the onset gains more strength with a maximum that extends radially from the suction surface hub edge to the blade mid section and beyond. The right column shows the vorticity distribution for the new endwall case. As seen, the vorticity distributions generated by the new method has lower strength than the reference case. This is true for all three axial positions shown in Fig. 16.

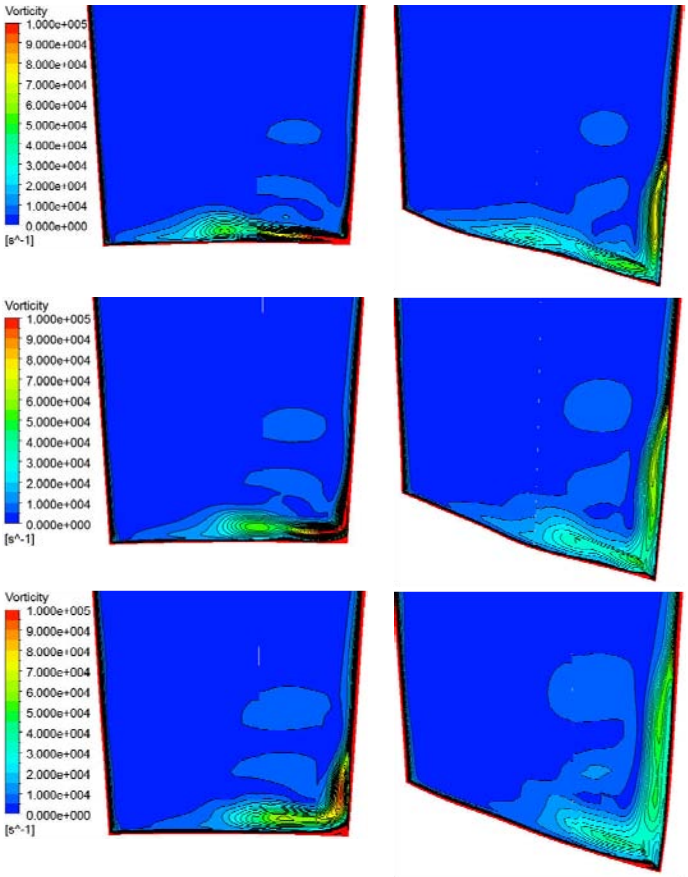

Fig. 16: Vorticity distribution in the passage

Reference case (left) at:	New Case (right) at:
x= 0.30C_{ax} (top)	x= 0.30C_{ax} (top)
x= 0.42C_{ax} (middle)	x= 0.42C_{ax} (middle)
x= 0.55C_{ax} (bottom)	x= 0.55C_{ax} (bottom)

CONCLUSIONS, ONGOING WORK

A new method for designing non-axisymmetric endwall contours is presented. It is based on continuous diffusion process and utilizes a prescribed deceleration of the secondary flow velocity from pressure to suction surface. By defining a target pressure and constructing the endwall contour, it was shown that the pressure difference on the hub can be controlled reducing the secondary flow and increasing the efficiency. This method can equally be applied to HP-, IP-, and LP- turbines and compressors regardless of the load coefficient, flow coefficient and degree of reaction. It is strongly physics based, very straight forward and easy to use. The method was applied to the second rotor of the TPFL-turbine, where on the first attempt the prescribed target pressure covered only the critical portion of the hub with a strong secondary flow movement. The rotor efficiency has increased from 88.82% in reference case to 89.33% for the new contoured case. Further improvement is expected by extending the target pressure from the blade inlet to the exit. A marginal efficiency improvement of 0.16% was also achieved by filleting the leading edge. This improvement, although marginal, if combined with the endwall contouring may add additional 0.1% - 0.2% to endwall efficiency.

The ongoing and future work include: (a) extending the target pressure to cover the entire blade hub section, (b) implementation of the leading edge fillets, (c) designing endwall contour attachments to be inserted into the second rotor row for experimental validation and (d) inserting three sets of endwall contour attachments to the three-stage turbine and perform a complete performance and efficiency test.

ACKNOWLEDGMENT

The research work presented in this paper is part of a major research project sponsored by the United States Department of Energy. The authors would like to thank Mr. Richard Dennis, the Program Manager and Mr. Robin Ames, the Project Manager of the National Energy Technology Laboratory.

REFERENCES

[1] Schobeiri, M., 2004, "Turbomachinery Flow Physics and Dynamic Performance," a textbook in press by Springer-Verlag, Heidelberg, New York, Toronto, ISBN 3-540-22368-1.

[2] Traupel, W., "Thermische Turbomaschinen," Bd.I, 1977, Springer-Verlag, Berlin.

[3] Denton, J.D., "Loss Mechanisms in Turbomachines," ASME Journal of Turbomachinery, Vol.115, pp. 621-656 (1993).

[4] Sieverding C.H., 1985, "Recent Progress in the Understanding of Basic Aspects of Secondary Flows in Turbine," Blade Passages. ASME Transactions, Journal of Engineering for Gas Turbines and Power, Vol. 107, pp. 248-257 (April 1985).

[5] Langston, L.S., 2001, "Secondary Flows in Axial Turbines-A Review," Annals of the New York Academy of Sciences, Vol. 934, pp. 11-26.

[6] Schobeiri, M.T., Gilarranz, J., and Johansen, E., "Final Report on: Efficiency, Performance, and Interstage Flow Field Measurement of Siemens-Westinghouse HP-Turbine Blade Series 9600 and 5600," September, 1999.

[7] Schobeiri, M.T., Gillaranz, J. L., and Johansen, E.S., 2000, "Aerodynamic and Performance Studies of a Three Stage High Pressure Research Turbine with 3-D Blades, Design Point and Off-Design Experimental Investigations," Proceedings of ASME Turbo Expo 2000, 2000-GT-484.

[8] Schobeiri, M.T., Suryanaryanan, A., Jerman, C., and Neuenschwander, T., 2004, "A Comparative Aerodynamic and performance study of a three-stage high pressure turbine with 3-D bowed blades and cylindrical blades," Proceedings of ASME Turbo Expo 2004 Power of Land Air and Sea, June 14 - 17, 2004, Vienna, Austria, paper GT2004-53650.

[9] Chibli, H., Sherif A., and M.T. Schobeiri, 2009, Proceedings of ASME Turbo Expo 2009 June 18-12, Orlando Florida, GT-2009-59131.

[10] Sauer, H., Wolf, H., "The Influence of the Inlet Boundary Layers on the Secondary Losses of Turbine Stages", AGARD-Conference Proceedings537, Montreal, Canada Oct.1993.

[11] Sauer, H., Wolf, H., "Influencing the Secondary Flow in Turbine Cascades by the Modification of the Blade Leading Edge", 2. European Conference on Turbomachinery, Antwerpen 1997.

[12] Sauer, H., Wolf, H., and Vogeler, K., 2000, "Reduction of Secondary Flow Losses in Turbine Cascades by Leading Edge Modifications at the Endwall", ASME-2000-GT-0473.

[13] Zess, G. A. and Thole, K. A., 2001, "Computational Design and Experimental Evaluation of Ising A Leading Edge Fillet on a Gas Turbine Vane," Proceedings of ASME Turbo Expo 2001, 2001-GT-0404.

[14] Becz, S., Majewski, M.S., and Langston, L.S., 2003, "Leading Edge Modification Effects on Turbine Cascade Endwall Loss," Proceedings of ASME Turbo Expo 2003, 2003-GT-38898.

[15] Hartland, J., and Gregory-Smith, D., 2002, "A Design Method for the Profiling of End Walls In Turbines," ASME, GT-2002-30433, Proceedings of ASME Turbo Expo 2002, June 3–6, 2002, Amsterdam, The Netherlands.

[16] Ingram, G., Gregory-Smith, D.G., Rose, M., Harvey, N., and Brennan, G., 2002, "The Effect of End-Wall Profiling on Secondary Flow and Loss Development in a Turbine Cascade," Proceedings of ASME Turbo Expo 2002, 2002-GT-30339.

[17] Eymann, S., Reinmöller, U., and Niehuis, R., 2002, "Improving 3d Flow Characteristics in a Multistage Lp Turbine by Means of Endwall Contouring and Airfoil Design Modification –Part 1: Design and Experimental Investigation," Proceedings of IGTI'02 ASME Turbo Expo 2002, 2002-GT-30352.

[18] Sauer, H., Müller, R., and Vogeler, K., 2000, "Reduction of Secondary Flow Losses in Turbine Cascades by Leading Edge Modifications at the Endwall," May 8-11, 2000, Munich Germany, 2000-GT-0473.

[19] Ingram, G., Gregory-Smith, D.,Rose, M., N. Harvey, N. and Brennan, G., 2002, "The Effect of End-Wall Profiling on Secondary Flow and Loss Development in a Turbine Cascade," Proceedings of ASME Turbo Expo 2002, GT-2002-30339.

[20] Ingram, G. Gregory-Smith, D. and Harvey, N., "Investigation of a Novel Secondary Flow Feature in a Turbine Cascade with End Wall Profiling," Proceedings of ASME Turbo Expo 2004, GT2004-53589.

[21] Saha, A.K., and Acharya, S., 2006, "Computations of Turbulent Flow and Heat Transfer through a Three-Dimensional Non-Axisymmetric Blade Passage," Proceedings of ASME Turbo Expo 2006, GT2006-90390.

[22] Praisner, T. J., Allen-Bradley, E., Grover, D. C. Knezevici and Sjolander, S. A., 2007, "Application of Non-Axisymmetric Endwall Contouring to Conventional and High-Lift Turbine Airfoils," Proceedings of ASME Turbo Expo 2007, GT2007-27579.

[23] Harvey, N. W., Rose, M. G. , Taylor, M. D.S. Shahpar, J., Harland and D. G. Gregory-Smith, 2000, "Nonaxisymmetic Turbine End Wall Design: Part I: Three-Dimensional Linear Design System," Journal of Turbomachinery, Vol. 122, pp 278-285.

[24] J. C. Harland, D. G. Gregory-Smith, N. W. Harvey and M. G. Rose, 2000, "Nonaxisymmetic Turbine End Wall Design: Part II – Experimental Validation," Journal of Turbomachinery, Vol. 122, pp 286-293.

[25] G. Brennan, N. W. Harvey, M. G. Rose, N. Fomison and M. D. Taylor, 2001, "Improving The Efficiency of The Trent 500 HP Turbine Using Non-Axisymmetric End Walls: Part 1 Turbine Design," Proceedings of ASME Turbo Expo 2001, 2001-GT-0444.

[26] N. W. Harvey, M. G. Rose, G. Brennan and D. A. Newman, 2002, "Improving Turbine Efficiency Using Non-Axisymmetric End Walls: Validation in The Multi-Row Environment and with Low Aspect Ratio Blading," Proceedings of ASME Turbo Expo 2002, GT-2002-30337.

[27] T. Germain, M. Nagel, I. Raab, P. Schuepbach, R. S. Abhari and M. Rose, 2008, "Improving Efficiency of a High Work Turbine Using Non-Axisymmetric End Walls Part I: Endwall Design and Performance," Proceedings of ASME Turbo Expo 2008, GT2008-50469.

[28] G. Snedden, D. Dunn, G. Ingram and D. Gregory-Smith, 2009, "The Application of Non-Axisymmetric Endwall Contouring in a Single Stage, Rotating Turbine," Proceedings of ASME Turbo Expo 2009, GT2009-59169.

[29] G. Snedden, D. Dunn, G. Ingram and D. Gregory-Smith, 2010, "The Performance of a Generic Non-Axisymmetric End Wall in a Single Stage, Rotating Turbine at On and Off-Design Conditions," Proceedings of ASME Turbo Expo 2010, GT2010-22006.

[30] Schobeiri, M.T., 2010, "Fluid Mechanics for Engineers, A Graduate Textbook, Springer Verlag, ISBN978-3-642-11593-6.

[31] Schobeiri, M.T. 1979, " Theoretische und experimentelle Untersuchungen laminarer und Turbulenter Strömungen in Diffusoren, Dissertation, Technische Hochschule Darmstadt, D17.